Human Movement Science 68 (2019) 102528

Contents lists available at ScienceDirect

Human Movement Science

journal homepage: www.elsevier.com/locate/humov

Full Length Article

Characterization of statistical persistence in joint angle variation during walking

Dorothea J. Tsang, Meghan Lukac, Anne E. Martin*

Department of Mechanical Engineering, The Pennsylvania State University, University Park, PA 16802, USA

A R T I C L E I N F O

Keywords:
Hurst exponent
DFA
Joint angle
Noise
Gait

A B S T R A C T

The objective of this study was to characterize joint angle variation across strides. Specifically, the statistical persistence of variations were quantified using the Hurst exponent. If a time series exhibits statistical persistence, then a parameter which is smaller (or larger) than average will tend to be followed by additional values that are also smaller (or larger) than average. Human walking has statistical persistence between stride durations. Variation in stride duration must arise from variation in the motion of the leg segments during walking. It is unclear, however, if the joint angle variation also exhibits statistical persistence. This study examined kinematic data collected from nine healthy adults walking for 10 min at a self-selected comfortable speed on a treadmill. The joint angle variation in the lower limbs was parameterized using first-order Fourier series which in turn were described by frequency and magnitude coefficients for each stride. To determine if the joint angle variation exhibited statistical persistence, the Hurst exponent was found for each coefficient at each joint. The mean Hurst exponents were 0.54 for the frequency coefficients and 0.61 for the magnitude coefficients. Neither the frequency or magnitude coefficients exhibited statistically significant persistence, although some of the magnitude coefficients were close to reaching statistical significance. This suggests that joint angle variability in healthy adults does not directly produce the statistical persistence observed in stride duration fluctuations.

1. Introduction

Hausdorff, Peng, Ladin, Wei, and Goldberger (1995) study on human walking variability quantified and modeled stride interval fluctuations, revealing the existence of statistical persistence within them. Having statistical persistence means that if the duration of one stride is smaller than average, then the durations of the subsequent strides are also likely to be smaller than average. Similarly, if the duration of one stride is longer than average, subsequent stride durations are also likely to be longer. The existence and magnitude of statistical persistence are typically found using detrended fluctuation analysis (DFA) to compute the Hurst exponent H. A Hurst exponent of < 0.5 indicates an anticorrelated, antipersistent structure. A Hurst exponent of ≈ 0.5 indicates white noise and no correlation between values. A Hurst exponent of > 0.5 indicates persistent correlations (Ihlen, 2012). Many studies have confirmed that statistical persistence exists in stride interval fluctuations (Bollens, Crevecoeur, Detrembleur, Guillery, & Lejeune, 2012; Dierick, Nivard, White, & Buisseret, 2017; Rhea, Kiefer, D'Andrea, Warren, & Aaron, 2014; Warlop, Detrembleur, Stoquart, Lejeune, & Jeanjean, 2018). This persistence in stride duration was found to be altered with age and some diseases (Hausdorff, 2007; Warlop et al., 2018). Gender also appears to play a role, as women exhibit greater variability than men in spatial-temporal gait parameters,

* Corresponding author.
E-mail address: aem34@psu.edu (A.E. Martin).

https://doi.org/10.1016/j.humov.2019.102528
Received 28 March 2019; Received in revised form 2 August 2019; Accepted 1 October 2019
Available online 06 November 2019
0167-9457/

even after normalizing for height (Yamasaki, Sasaki, & Torii, 1991).

An alternative view of statistical persistence and anti-persistence is that it quantifies how tightly regulated a quantity is (Dingwell & Cusumano, 2010). In an anti-persistent time series, differences from the mean are typically over corrected at the next instant, indicating tight regulation. In contrast, persistence indicates loose regulation because differences from the mean are typically not corrected quickly. Human gait exhibits both statistical persistent and anti-persistence simultaneously. For treadmill walking without a metronome, stride intervals and position on the treadmill both exhibit statistical persistence while stride speed exhibits statistical anti-persistence (Dingwell & Cusumano, 2010, 2015). When a metronome is introduced, humans alter the statistical properties of their stride interval fluctuations to match the statistical properties of the metronome beat (Roerdink, Daffertshofer, Marmelat, & Beek, 2015; Roerdink, de Jonge, Smid, & Daffertshofer, 2019). Together, these results suggest that the statistical properties of stride-to-stride fluctuations may represent how tightly regulated a particular quantity is.

For either interpretation, changes in statistical persistence of gait variability from normal for a particular condition may be useful in isolating changes in the body related to age and identifying the onset of pathologies that affect locomotor control. To date, only spatiotemporal quantities have been examined for statistical (anti-)persistence. However, fluctuations in spatiotemporal quantities must arise from fluctuations in joint kinematics. The purpose of this study is to determine if variations in joint kinematics also exhibit a statistical structure. Specifically, this study examines if statistical persistence exists in the joint angles of the hip, knee, and ankle during treadmill walking in healthy adults.

Some studies have begun to explore how the fluctuations in stride duration are affected by the control systems (Bollens, Crevecoeur, Detrembleur, Warlop, & Lejeune, 2014; Dingwell & Cusumano, 2015; Dingwell, Salinas, & Cusumano, 2017) and natural dynamics (Ahn & Hogan, 2015; Dingwell & Marin, 2006) of the body. One source of the variation comes from low-level central nervous system processes involving the spinal and supraspinal networks (Bollens et al., 2014) which explains the link between neurological disorders and changes in gait such as decreased walking speed and increased variability (Hausdorff, 2007; Moon, Sung, An, Hernandez, & Sosnoff, 2016; Warlop et al., 2018). Speed, which affects both gait kinematics and kinetics (Schwartz, Rozumalski, & Trost, 2008), also impacts stride interval fluctuations. This may partly be because humans appear to prioritize speed control over position control (Dingwell & Cusumano, 2015). Changes in speed also alter the variability of some joint angles (Kang & Dingwell, 2008) as the neuromuscular system encounters increasing constraints and coordination problems at walking speeds slower or faster than is comfortable (Jordan, Challis, & Newell, 2007). Since joints in the lower body may be moved in multiple ways to accomplish the same stride duration and because statistical persistence appears to strengthen for stride duration at non-preferred speeds (Jordan et al., 2007), there is value in examining the variability in joint angles to understand what is typical at preferred walking speeds. This will allow comparisons of joint angle variability between healthy individuals and individuals with impaired gait and could potentially result in improved fall risk measures.

Initial models of joint angle variation used nonlinear dimensionality reduction techniques (Dingwell & Cusumano, 2000; Zhang, Zhang, Feng, & Small, 2010). However, these models do not illustrate the variation as a function of time. This can be addressed with a low-order Fourier series (Martin, Villarreal, & Gregg, 2016). For this paradigm, the joint angle variation is described by frequency and magnitude coefficients. Each step has a unique set of coefficients. The standard deviations of the coefficients indicate similar degrees of variation across the major joints of the lower body: the hip, knee, and ankle joints (Martin et al., 2016). This is consistent with studies that have looked at the standard deviations of the angles directly without considering the structure of the variability (McGinley, Baker, Wolfe, & Morris, 2009).

This study examined the joint angle variability of healthy adults during treadmill walking. DFA was be applied to the frequency and magnitude coefficients from the Fourier series to determine if statistical persistence existed in the joint angle variability. This study into the variances in lower limb joint angles provides baseline data for healthy adult gait for future comparisons to gait patterns of older adults and patients with gait impairments and higher fall risk.

2. Methods

Ten healthy adults (5 females, 5 males, mass: 66.9 ± 13.7 kg, height: 1.71 ± 0.11 m, leg length: 0.86 ± 0.062 m) participated in the experiment. Due to data collection issues, the data from one male subject could not be used, so the analysis was performed using the remaining nine subjects. Prior to the experiment, each subject provided informed consent. Subjects all had a BMI of less than 30 and were between 18 and 40 years old. Potential subjects were excluded if they had any self-reported conditions that affected their walking ability. One subject expressed existing pain in their ankle from an unrelated injury before the experiment, however the pain did not hinder their ability to walk normally. This was confirmed via visual inspection.

Sixteen reflective markers for the standard Plug-in Gait lower body marker set (Vicon, 2018a) were placed on the subjects' hips, legs, ankles, and feet prior to walking. Subjects wore their own shoes that they considered comfortable to walk in.

Each subject walked on a split-belt instrumented treadmill (Bertec, Columbus, OH) for a single ten-minute trial at a comfortable speed (1.04 ± 0.14 m/s) averaging 538 strides. To determine the appropriate speed prior to data collection, the subject walked on the treadmill while the speed was adjusted until they decided they would be able to comfortably walk at their chosen speed for ten minutes. During data collection, fourteen cameras (Vicon, Oxford, UK) surrounding the treadmill recorded marker positions at 100 Hz. Ground reaction force data were recorded at 1000 Hz using the force plates embedded in the treadmill.

After the experiment, all data were processed using Nexus Software (Vicon, Oxford, UK) with the Plug-in Gait model and standard filtering parameters. In order to fill the gaps in the recorded data due to marker occlusion, the number of frames per gap was considered. Gaps of less than 20 frames were filled using the cyclic method included in Nexus. The cyclic method identifies regions that are similar in other cycles and fills the gap using those marker positions (Vicon, 2018b). Longer gaps were filled using the spline method which applies a cubic spline interpolation method to the frames with gaps. For each subject, an average of 20–60 gaps needed to be filled, with the exception of two trials in which the longest gap exceeded 100 frames. However, this was still a very small fraction of the 60,000 frames collected over the ten-minute trial. The resulting raw data were further analyzed with Matlab.

Data were split into full strides, from heel strike to heel strike. A combination of two methods was used to identify heel strike because neither method consistently identified all heel strikes. When a subject stepped cleanly onto the force plates, heel strike time was identified using the vertical GRF. To do so, a threshold was set based on a percentage (1%) of the subject's weight to detect when a leg was in the swing period. When the vertical ground reaction force was less than 1% of the subject's weight, the leg was assumed to be in swing. Heel strike was determined to have occurred when the force crossed from just below the threshold to just above the threshold. A second method using foot marker positions (O'Connor, Thorpe, O'Malley, & Vaughan, 2007) was also used to find heel strike times. Briefly, the foot vertical velocity was found by averaging the vertical position of the toe and heel markers and then differentiating. The local minima of the foot velocity was found. Every gait cycle, there is one large local minima and multiple smaller local minima. Heel strike was identified by starting at the large local minima and checking each successive local minima until the heel was close to the ground. The time of this local minima was identified as heel strike. Once heel strike for a particular gait cycle was found, the algorithm jumped to the next large local minima and repeated the search procedure. To combine the heel strike times from the two methods, the average of the two methods was used when both methods correctly identified heel strike. When only one method correctly identified heel strike, the time of that method was used. Using this combined method eliminated the need for manual identification of heel strike times.

For each joint and side, the joint trajectory was decomposed into a per-subject mean plus the variation. To do so, the joint angle data for each stride were interpolated over 1000 equally-spaced time points. These time points were normalized so that 0 and 1 corresponded to the heel strikes at the start and end of the stride respectively. The per-subject mean was found for each time point by averaging across all strides. The joint variation was calculated by subtracting the mean angle from the total angle for each stride (Fig. 1(a)). Then, for each stride, a Fourier series was fit to the variation to give a unique set of coefficients that described the within-stride variation (Fig. 1(b)). For this work, a first-order Fourier series was used:

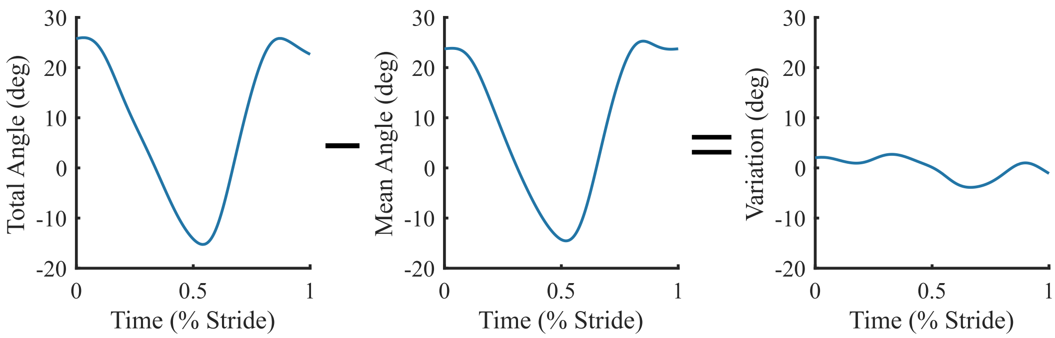

(a)

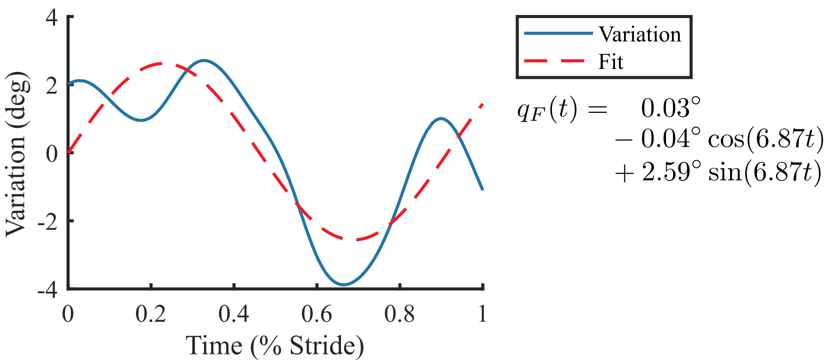

(b)

Fig. 1. (a) The joint angle variation is the total joint angle minus the mean angle. The variation is found separately for each subject, joint, and side. These plots show a representative stride from one subject's left hip. In all cases, the variation appears to be approximately sinusoidal. (b) The joint angle variation is described by fitting a first-order Fourier series to it. The best-fit Fourier series for this particular stride is given by the equation shown in the figure. The best-fit Fourier series is determined for each stride to find the unique set of coefficients that describes the variation in that stride.

$$q_{Fij}(t) = a_{0ij} + a_{1ij}\cos(\omega_{ij}t) + b_{1ij}\sin(\omega_{ij}t) \tag{1}$$

where q_{Fij} is the variation from the mean, ω_{ij} is the frequency coefficient, and a_{0ij}, a_{1ij}, b_{1ij} are the magnitude coefficients, all for stride i of joint j. Since every stride has a different variation trajectory, a different set of coefficients was found for every stride. All of the coefficients have physical meaning. The a_0 coefficient shifts the entire curve to cause more or less joint flexion. Together, the a_1 and b_1 coefficients define the amplitude and phase shift of the variation. The frequency coefficient controls how many cycles of variation occur in one stride. Because of the way variation was defined, the mean values for the magnitude coefficients were zero. If $a_{0ij} = a_{1ij} = b_{1ij} = 0^\circ$ for stride i of joint j, the best-fit curve for the variation would be a straight line at 0°. This indicates that the total angle would match the mean angle to within the accuracy of the fit. The objective of this paper was to determine if there was a consistent pattern to these coefficients or if they could be represented as independent draws from a normal distribution, suggesting that they arise purely due to noise.

The Fourier series were found using the Matlab function 'fit' with the default options. This method uses nonlinear least squares to find the coefficients. Because this is a form of optimization, the function sometimes exploits the computer's numerical precision and finds extremely large magnitude coefficients ($\gg$1000°). To deal with this, Martin et al. (2016) found the fits without bounding the magnitude coefficients and then discarded any fits with a magnitude coefficient above three standard deviations from the mean. This would not work here because it is critical to keep all strides to maintain the integrity of the time series. It was also important to eliminate outliers that do not truly represent the data to avoid underestimating the Hurst exponent (Achard & Coeurjolly, 2010; Nelson, Nafornita, & Isar, 2015). To deal with this, we chose to bound the magnitude coefficients at ± 3° because it was 2.5 times the magnitude coefficient standard deviation found by Martin et al. (2016) and because it removed all of the obvious outliers without causing obvious saturation of the coefficient values. We are confident that these bounded Fourier series fits are truly representative of the data in a way that the unbounded fits are not for several reasons. 1) It is well known that optimization methods will exploit loopholes to obtain slightly better results while generating infeasible solutions when constraints are not placed appropriately. When the coefficients were not bounded, some strides had magnitude coefficients $\gg$1000°, which has no physical meaning. This type of observed behavior is a common sign that loopholes are being exploited. 2) When the coefficients were not bounded, the quality of the fit degraded significantly when the coefficients were rounded to a reasonable number of significant digits as opposed to keeping all digits to machine precision. This is another common sign that loopholes are being exploited. When the coefficients were bounded, rounding had no discernible effect on the quality of the fit. 3) The fits with and without bounds were very similar both visually and quantitatively. The differences in the R^2 values were on the order of 0.001 and differences in the RMSE values were on the order of 0.001°. This was within the range of expected experimental error.

Beyond determining how to bound Fourier series coefficients, there were some other some subjective choices. Martin et al. (2016) separated strides into their stance and swing periods, characterizing the stance period with a second-order Fourier series while characterizing the swing period with a first-order Fourier series. This gave fits with median R^2 values of 0.96 (hip), 0.93 (knee), and 0.89 (ankle), and median root mean square errors (RMSE) of 0.14° (hip), 0.28° (knee), and 0.27° (ankle). While this gave good quality fits, it also required a large number coefficients per stride. Further, using a different Fourier series order for stance and swing means that stance and swing coefficients could not be directly compared to each other. It also meant that two subsequent values of a particular coefficient did not directly follow each other in time because the stepping pattern alternates between stance and swing. Together, this makes interpretation of the results slightly more challenging. Using a single first-order Fourier series for the entire stride reduced both the quality of the fit and the number of coefficients required. Using a single first-order Fourier series for the entire stride gave median R^2 values of 0.73 (hip), 0.63 (knee), and 0.56 (ankle), and median RMSE of 0.45° (hip), 0.86° (knee), and 0.70° (ankle). Because the fit was over the entire stride, sequential coefficient values directly follow each other in time. An intermediate option is a third-order Fourier series fit over the entire stride. This resulted in goodness of fit values similar to those obtained when dividing the stride into stance and swing as in Martin et al. (2016). In contrast to Martin et al. (2016), sequential coefficient values directly follow each other in time. As shown later, the results for this paper are insensitive to the choice of fitting options, so we present detailed results for the simplest first-order fit over the entire stride and summary results for other options.

Because a separate fit was found for each stride, every stride had a unique set of coefficients. This resulted in a time series for each frequency and magnitude coefficient where the coefficients were sequentially ordered from the first stride to the last stride. The coefficients for each stride were then collectively analyzed to determine the presence of any persistent or antipersistent behavior.

To characterize the stride durations and joint angle variation, DFA was performed using standard methods (Ihlen, 2012). The time series of coefficients was converted into a random walk-like time series by first subtracting the mean and then calculating the cumulative sum X_n for each stride,

$$X_n = \sum_{k=1}^{n} s_k - \bar{s} \tag{2}$$

where s_k is a Fourier series coefficient for step k, and the overbar indicates the mean. The sequence of X_n values are stored in vector X. Then, X_n was divided into equal, non-overlapping segments and the local root-mean-square (RMS) value was computed:

$$RMS_i^2 = \overline{(X(v) - f(X(v))^2)} \tag{3}$$

where v is the segment and $f(X(v))$ is the linear regression line fit to X for segment v. The variation of the local RMS is quantified by an overall RMS, F.

$$F_i = \sqrt{\overline{RMS_i^2}} \tag{4}$$

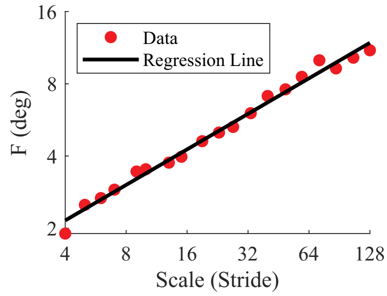

Fig. 2. Average overall RMS (F, Eq. 4) vs. segment size in log-coordinates for a representative subject's right ankle frequencies found using a first-order Fourier series over the entire stride with bounds at ± 3°. The Hurst exponent is 0.49 ($R^2 = 0.99$), indicating a time series in which consecutive values are not correlated with each other.

This was repeated 19 times with evenly-spaced (on a $\log_2$ scale) segment sizes ranging from 4 strides to 128 strides. Evenly spaced segment sizes provide a more accurate measure of the Hurst value than other methods (Almurad & Delignières, 2016). To find the Hurst exponent (H), the binary logarithm of the overall RMS and the segment size was calculated. A linear regression line was then fit to these data (Fig. 2). The Hurst exponent is the slope of that regression line. Since the subjects walked for 10 min and averaged 538 strides during that time, partitioning 538 strides into segments of more than 128 strides each would result in fewer than 4 segments, which is insufficient for accurately calculating the average RMS value. 19 segment sizes provided sufficient data to get a good fit. A Hurst exponent of < 0.5 indicates an antipersistent structure in which a value below the mean is typically followed by a value above the mean and vice versa. A Hurst exponent of 0.5 indicates white noise and no correlation between consecutive values. A Hurst exponent of > 0.5 indicates a persistent structure in which a value below (or above) the mean is typically followed by more values below (or above) the mean (Ihlen, 2012). In the context of control, a Hurst exponent of < 0.5 indicates tight regulation, a Hurst exponent of > 0.5 indicates loose regulation, and a Hurst exponent of approximately 0.5 indicates a lack of regulation (Dingwell & Cusumano, 2010; Roerdink et al., 2015). The Hurst exponent for each frequency and magnitude coefficient of each side and joint was calculated separately to determine if there was a structure to the joint-level variation. The data for the left and right sides were then combined because subjects walked symmetrically and values were very similar for both sides. The Hurst exponent for stride duration was also found.

For scales of 4 to 128 strides, the trend in F_i was well represented with a linear regression line. When the magnitude coefficients were bounded, R^2 was greater than 0.93 for all cases and the median R^2 value was 0.99. When the magnitude coefficients were not bounded, the R^2 values decreased. The minimum R^2 value was 0.06, the second smallest R^2 value was 0.21, and the median R^2 value was 0.93. At scales exceeding 128 steps, the points often deviated from the trend apparent at smaller scale segments, suggesting insufficient data for the larger scales. This occurred in most parameters for most of the subjects. This is expected due to insufficient data for the larger scales. As such, for consistent analysis across all subject data, scales of 4 to 128 steps were used for the DFA.

Since the calculated Hurst exponents of the frequency and magnitude coefficients were approximately 0.5 for all subjects and joints on both sides, they were tested for statistical significance. To do so, surrogate data were obtained by scrambling data for each coefficient time series using the randperm function in Matlab to remove the influence of sequential ordering (Hausdorff et al., 1995; Lancaster, Iatsenko, Pidde, Ticcinelli, & Stefanovska, 2018; Schreiber & Schmitz, 2000). DFA was then applied on the scrambled data to obtain Hurst exponents. This was repeated for a total of 250 iterations. To calculate significance, the Hurst exponents from the 250 scrambled data series plus the Hurst exponent from the actual data series were sorted in increasing numerical order (Schreiber & Schmitz, 2000). The Hurst exponent from the actual data was located in position c from the end (i.e., if the actual data had the largest Hurst exponent, $c = 1$). The p-value was then given by

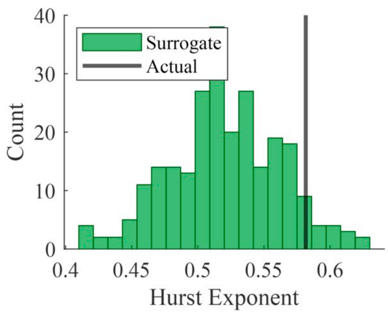

Fig. 3. Representative example of Hurst exponents calculated with surrogate data and with the actual data. The mean Hurst exponent for the surrogate data is 0.52; the actual Hurst exponent is 0.58, leading to a p-value of 0.08. In most cases for the magnitude coefficients, the actual Hurst exponent was greater than the mean of the surrogate Hurst exponents but less than the maximum surrogate Hurst exponent.

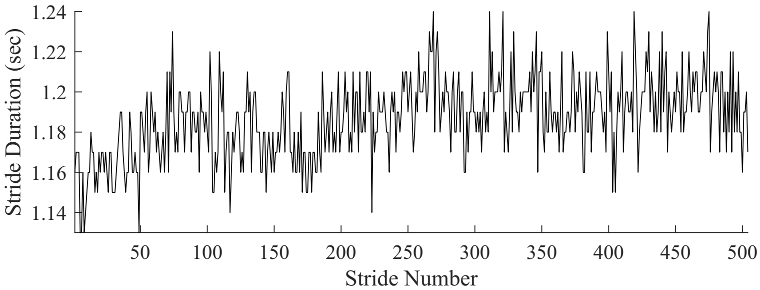

Fig. 4. Stride duration vs. stride number for a typical subject. As expected, the stride durations exhibits a persistent structure. The Hurst exponent for this data is 0.78.

$$p = \frac{c}{251}. \tag{5}$$

For each coefficient at each joint, there were a total of 18 actual Hurst exponents (nine subjects, two sides) and correspondingly 18 potentially different p-values. We used the median p-value to determine significance. We report both the median p-value and the number of cases (out of 18) in which the Hurst exponent was significantly above 0.5 based on Eq. 5. Significance was set at $\alpha = 0.004$ after Bonferroni correction. This corresponds to an overall significance level 0.05 of since there were twelve comparisons performed (four coefficients, three joints). To more fully characterize the data, we also report the number of cases in which the actual Hurst exponent was above the mean Hurst exponent for the surrogate data (Fig. 3). However, this is not used for statistical testing.

The code to find the joint variation and calculate the Hurst exponents is provided as supplementary material.

3. Results

3.1. Validation of data with stride duration results

As expected, stride duration exhibits persistent correlations as there are relatively long portions of the data in which all the strides have values either below or above the average (Fig. 4). The average Hurst exponent for stride duration for all subjects was 0.76 ± 0.12, which is within the range reported in other studies (Bollens et al., 2012; Dierick et al., 2017; Rhea et al., 2014; Warlop et al., 2018).

3.2. Joint angle variability results

In contrast to stride duration, the frequency coefficients for joint angle variation appeared to vary randomly (Fig. 5). The mean Hurst exponent across all subjects, sides, and joints was 0.54, which was not statistically different from the surrogate data (Fig. 6, Table 1). The median Hurst exponent for the surrogate data was 0.52. Only 65% of the actual Hurst exponents were greater than the mean of their respective surrogate's Hurst exponent.

For the a_0 magnitude coefficients, there were more noticeable portions of the data with values either all below or all above the average (Figs. 6 and 7, Table 1). The Hurst exponents were larger than for frequency but smaller than for stride duration, with a mean value of 0.66. The mean value of the Hurst exponent for the surrogate data was 0.52. The actual data was statistically different than the surrogate data for the hip, and almost reached statistical significance for the knee and ankle. Just over half (59%) of the individual cases were statistically different from their respective surrogate data. A case is a single subject for a single side. 96% of the actual Hurst exponents were greater than the mean of their respective surrogate's Hurst exponent. For the a_1 and b_1 magnitude

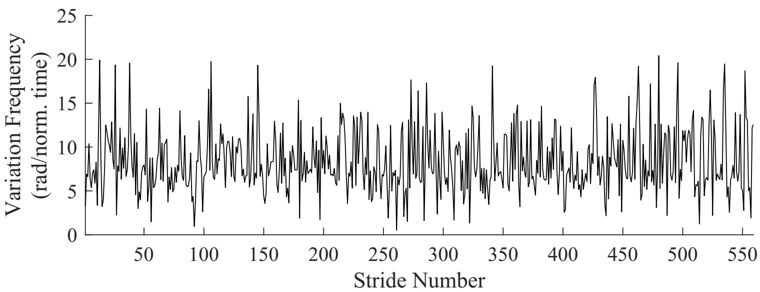

Fig. 5. The joint angle variation frequency (ω, Eq. 1) for a representative subject's the right hip joint appears to have no long portions of data where all values are above or below the mean, suggesting random behavior. The Hurst exponent for this data is 0.53.

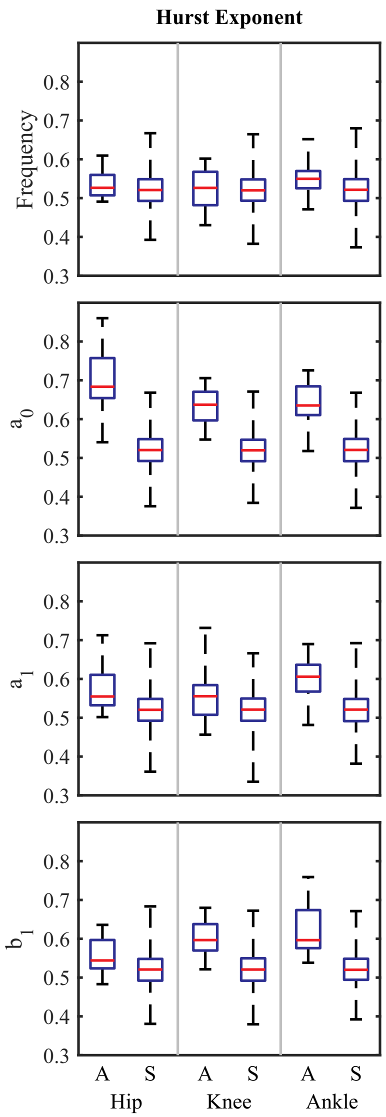

Fig. 6. Hurst exponents for the frequency and magnitude coefficients of the variation for the hip, knee, and ankle joints for all subjects. The joint variation was fit using a first-order Fourier series over the entire stride with bounds on the magnitude coefficients of ± 3°. Hurst exponents for both the actual (indicated with "A") and surrogate (indicated with "S") data are shown. For the frequency coefficients, the actual and surrogate data had very similar Hurst exponents. For the magnitude coefficients, the Hurst exponents for the actual data were typically greater than the median but smaller than the maximum Hurst exponent for the surrogate data.

coefficients, the data appeared to vary randomly or exhibit slight statistical persistence. The mean Hurst exponent was 0.58 for the actual data and 0.52 for the surrogate data. Overall, the actual data was not statistically different from the surrogate data, although just over one third (39%) of the individual cases were statistically different from the surrogate data. Further, 87% of the actual Hurst exponents were greater than the mean of their respective surrogate's Hurst exponent.

3.3. Effect of fitting choices

To ensure that our results were insensitive to our choices regarding fitting the joint variation, we calculated the Hurst exponents using a total of five fit types:

1. Fitting the entire stride using a first-order Fourier series with bounds on the magnitude coefficients of ± 3° (what is presented in this paper),
2. Fitting the entire stride using a first-order Fourier series with no bounds on the magnitude coefficients,
3. Fitting the entire stride using a third-order Fourier series with bounds on the magnitude coefficients,

Table 1
Mean ± one standard deviation for the Hurst exponents for the actual data (H), median p-value, number of cases (out of 18) in which the Hurst exponent is significantly greater than the surrogate data (# Sig.), and number of cases (out of 18) in which the actual Hurst exponent is greater than the mean Hurst exponent of the surrogate data (# > H_S). For all coefficients, the mean Hurst exponent for the surrogate data is 0.52 ± 0.04. All values are for joint variation fits over the entire stride using a first-order Fourier series with bounds on the magnitude coefficients at ± 3°.

Coefficient	**H**	**p**-value	# Sig.	# > $\mathbf{H_S}$
Hip				
ω	0.54 ± 0.04	0.410	0	11
a_0	0.70 ± 0.09	0.004	14	18
a_1	0.57 ± 0.06	0.195	4	15
b_1	0.56 ± 0.05	0.259	1	14
Knee				
ω	0.52 ± 0.05	0.474	0	10
a_0	0.63 ± 0.05	0.006	9	18
a_1	0.56 ± 0.06	0.203	2	13
b_1	0.60 ± 0.05	0.062	5	18
Ankle				
ω	0.55 ± 0.05	0.315	1	14
a_0	0.64 ± 0.06	0.006	9	16
a_1	0.60 ± 0.06	0.032	4	16
b_1	0.62 ± 0.06	0.036	5	18

4. Fitting the stance period with a second-order Fourier series and the swing period with a first-order Fourier series with bounds on the magnitude coefficients of ± 3°, and
5. Fitting the stance period with a second-order Fourier series and the swing period with a first-order Fourier series with no bounds on the magnitude coefficients (this is closest to what Martin et al. (2016) did).

There was almost no difference in the Hurst exponent for the frequency coefficients for any of the fit types tested (Table 2). In all cases, the a_0 coefficients had the largest mean Hurst exponent. When the magnitude coefficients were bounded, the Hurst exponent for a_0 was much larger than the other magnitude coefficients. When the magnitude coefficients were not bounded, the Hurst exponent for a_0 was slightly larger than the other magnitude coefficients. This is the largest effect that any of the fitting choices had. The Hurst exponents for the remaining magnitude coefficients only exhibited small changes with different fit types.

4. Discussion

As expected, these data support previous findings that stride duration exhibits statistical persistence. The average Hurst exponents found in other studies ranged from 0.73 to 0.83. The average Hurst exponent of the stride duration for these subjects was 0.76, which is in the previously reported range.

The frequency coefficients of the joint angle variation does not appear to exhibit either statistical persistence or anti-persistence. Instead, it exhibits a white noise-like behavior which means that the frequency coefficient for the previous stride has little to no influence on the frequency coefficient for the current step. The behavior was similar for all three leg joints. These findings may be in contrast to results found by Chung and Wang (2010) where the hip and knee joints were most affected by walking speed whereas the ankle joint was not affected by speed, gender, or age. Based on the results in Chung and Wang (2010), the expectation would be that hip and knee joints function similarly while the ankle joint behaves differently. It also suggests that the hip and knee joint angles are more likely to have statistical structure than the ankle joint angles since they were more sensitive to changes than the ankle joint was. While we did not explicitly alter gait, small perturbations occur every step and it seems reasonable to assume that compensation to these small perturbations may be similar to compensations to larger perturbations. The difference between the results of this study and those of Chung and Wang (2010) may be contributed to the latter analyzing average values while this study examined variability, which is more similar to the work of Kang and Dingwell (2008) who also examined changes in joint angles at different walking speeds and ages. Their results indicated greater variation in the hip angles in young adults and greater variation in the knee angles in older adults. However, the differences were not statistically significant. Similar to Chung and Wang (2010), this could suggest that there are some similarities in the behaviors exhibited by the hip and knee joints and that they are more sensitive to changes. However, other studies have found that age-related changes in gait occurred most strongly in the ankle joint and least strongly in the knee joint (Cabell, Pienkowski, Shapiro, & Janura, 2013). The results of this present study show that none of the joint angle frequency fluctuations had correlations between strides, which suggests that all joints are regulated similarly, at least with respect to frequency. Thus, this work partly agrees with the results in Chung and Wang (2010) and Kang and Dingwell (2008) because the hip and the knee joints function similarly. Given the differing conclusions from these various studies, further examinations into joint angles, perhaps with a larger sample size, are certainly required to better understand what typical behavior is for each leg joint.

The magnitude coefficient a_0 showed the strongest statistical persistence of all the coefficients, although it did not quite reach statistical significance for the knee or ankle. This is not surprising because the a_0 coefficient represents a constant offset from the mean joint trajectory. Given that the total joint trajectory must be continuous between steps, it seems reasonable for there to be periods in which the total joint trajectory is greater than or less than the mean joint trajectory, which would generate statistical

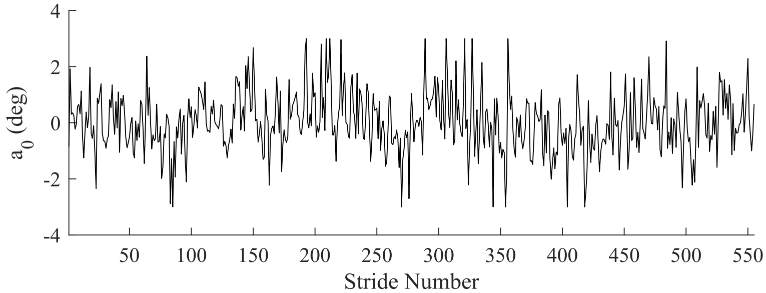

(a)

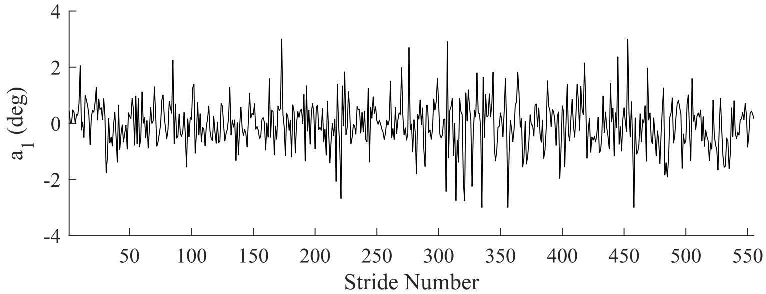

(b)

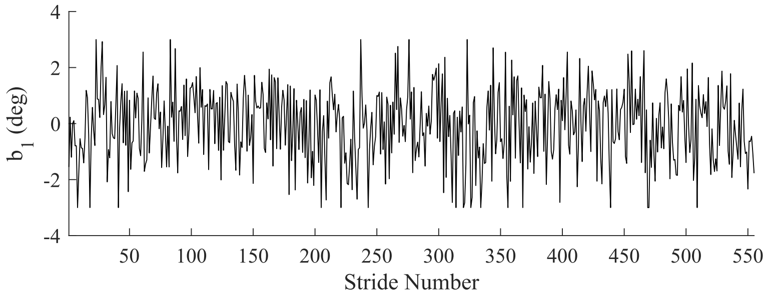

(c)

Fig. 7. The joint angle variation magnitude coefficients (Eq. 1) for a representative subject's right hip. The Hurst exponents were 0.70 for a_0, 0.52 for a_1, and 0.61 for b_1. As was typical for most subjects, the a_0 coefficient had noticeable segments of time where the values were either all above or below the mean, indicating statistical persistence and loose regulation. This persistence was weaker than for stride durations, however (compare with Fig. 4). In contrast, the a_1 and b_1 coefficients appeared to vary approximately randomly although they may have slight statistical persistence.

Table 2
Mean ± standard deviation of Hurst exponents for five different methods of fitting the joint variation. The a_0 column gives values for all a_0 magnitude coefficients, the Higher Mag. column gives values for all other magnitude coefficients (a_1, b_1, a_2, b_2, a_3, and b_3 as appropriate), and the Frequency column gives values for all frequency coefficients.

Period	Order	Bounds	Mean hurst exponent		
			a_0	Higher mag.	Frequency
Whole stride	1	± 3°	0.66 ± 0.07	0.58 ± 0.06	0.54 ± 0.05
Whole stride	1	No	0.57 ± 0.14	0.56 ± 0.12	0.53 ± 0.04
Whole stride	3	± 3°	0.65 ± 0.06	0.57 ± 0.06	0.53 ± 0.04
Stance & Swing	2 (stance) & 1 (swing)	± 3°	0.63 ± 0.06	0.59 ± 0.06	0.53 ± 0.04
Stance & Swing	2 (stance) & 1 (swing)	No	0.54 ± 0.09	0.54 ± 0.09	0.54 ± 0.05

persistence in the a_0 coefficient. The strongest persistence was at the hip joint while the knee and ankle joint were similar to each other. The magnitude coefficients a_1 and b_1 had similar Hurst exponent values that indicated either uncorrelated behavior or possibly weak statistical persistence. Given that a_1 and b_1 serve similar functions in a Fourier series, it is not surprising that they have similar Hurst exponents. Similar to frequency, the values were similar for all joints.

None of the coefficients exhibited as strong statistical persistence as stride duration, and almost none of the coefficients exhibited statistically significant persistence. Thus, statistical persistence in joint angles does not appear to directly cause statistical persistence in stride duration. Given that simple models of biped walking can exhibit statistical persistence in stride duration when the push-off magnitude is randomly varied (Ahn & Hogan, 2013; Gates, Su, & Dingwell, 2007), this is perhaps not surprising. Further, a very simple passive biped model that walks down a slope exhibits apparent chaos for some slope angles (Garcia, Chatterjee, Ruina, & Coleman, 1998). Thus, having statistical persistence in the input fluctuations is not required to obtain statistical persistence in stride fluctuations. The logical interpretation of this is that random noise in the neuromuscular system causes approximately random and uncorrelated variation in joint angles (Faisal, Selen, & Wolpert, 2008). Because muscles and tendons function much like a spring-damper system (Zajac, 1989), it is not surprising that they filter noise into approximately sinusoidal fluctuations that can be described by a Fourier series (Sinha, 2010). The physics of walking then convert this random noise into statistical persistence in stride duration. Since the variability is not controlled, this would explain why increased variability is correlated with increased fall risk (Hausdorff, Rios, & Edelberg, 2001).

However, this interpretation does not explain why humans can alter the statistical characteristics of stride duration (Roerdink et al., 2015, 2019). One alternative explanation is that walking is coordinated such that random fluctuations in input do not significantly affect important output dynamics (Diniz et al., 2011). Since our subjects did not have to meet any timing constraints, they could use their typical motion. If this explanation is true, adding a timing constraint via a metronome should alter the statistical characteristics of at least some of the joint angle variation coefficients because subjects must alter their coordination to meet the timing constraint. Another alternative explanation is that the magnitude coefficients are loosely regulated, and our statistical methods were unable to properly detect this. Given that the Hurst exponents for most of the magnitude coefficients were greater than both 0.5 and the mean of the surrogate data suggests that this may be true. Loose regulation of input fluctuations plus the physics of the system could be sufficient to alter the statistical properties of stride duration (Gates et al., 2007). Similar to the previous potential explanation, adding a timing constraint should alter the statistical characteristics of at least some of the joint angle variation coefficients.

This study was limited to examining only healthy adult subjects under 40 years old who walked on a treadmill. Results from overground walking may reveal stronger statistical persistence as the treadmill may have stabilized walking patterns (Dingwell & Cusumano, 2000; Hollman et al., 2015). Speed is also known to have a significant impact on the statistical persistence of stride duration fluctuations (Jordan et al., 2007; Kang & Dingwell, 2008; Schwartz et al., 2008). Future studies of joint angle variability at varying speeds may result in stronger persistence than observed at the preferred walking speed used in this study as stability decreases at increasingly non-preferred walking speeds (Jordan et al., 2007). Measuring joint angle variability in older adults may also reveal stronger statistical persistence since increased gait variability is often observed in older adults (Chung & Wang, 2010; Dingwell et al., 2017) even for those without diseases impacting locomotor control (Arnold, Mackintosh, Jones, & Thewlis, 2014; Dingwell et al., 2017). Since stride-to-stride error correction in older, healthy adults is not significantly different from that in young, healthy adults, compensation for the additional noise from aging could manifest itself in changes in walking style in order to gain additional stability (Dingwell et al., 2017). It may also be useful to examine if and how timing constraints alter the statistical characteristics of the joint angle variability.

Finally, how the variation in the continuous joint angle is converted into discrete values that can be used with DFA should be examined more carefully. It is possible that a Fourier series is not the appropriate method. However, Fourier series are often used to describe arbitrary signals and their coefficients have physically-meaningful interpretations, both of which support their use here. For the most part, the results appear to be insensitive to the exact details of the Fourier series, providing confidence in the results.

Funding

This research did not receive any specific grant from funding agencies in the public, commercial, or not-for-profit sectors.

Declaration of Competing Interest

None.

Appendix A. Supplementary data

Supplementary data to this article can be found online at https://doi.org/10.1016/j.humov.2019.102528.

References

Achard, S., & Coeurjolly, J.-F. (2010). Discrete variations of the fractional Brownian motion in the presence of outliers and an additive noise. *Statistics Surveys, 4*(1), 117–147.

Ahn, J., & Hogan, N. (2013). Long-range correlations in stride intervals may emerge from non-chaotic walking dynamics. *Public Library of Science ONE, 8*(9), e73239.

Ahn, J., & Hogan, N. (2015). Improved assessment of orbital stability of rhythmic motion with noise. *Public Library of Science ONE, 10*(3), e0119596.

Almurad, Z. M. H., & Delignières, D. (2016). Evenly spacing in detrended fluctuation analysis. *Physica A, 451*, 63–69.

Arnold, J. B., Mackintosh, S., Jones, S., & Thewlis, D. (2014). Differences in foot kinematics between young and older adults during walking. *Gait & Posture, 39*(2), 689–694.

Bollens, B., Crevecoeur, F., Detrembleur, C., Guillery, E., & Lejeune, T. (2012). Effects of age and walking speed on long-range autocorrelations and fluctuation

magnitude of stride duration. *Neuroscience, 210*(1), 234–242.
Bollens, B., Crevecoeur, F., Detrembleur, C., Warlop, T., & Lejeune, T. (2014). Variability of human gait: Effect of backward walking and dual-tasking on the presence of long-range autocorrelations. *Annals of Biomedical Engineering, 42*(4), 742–750.
Cabell, L., Pienkowski, D., Shapiro, R., & Janura, M. (2013). Effect of age and activity level on lower extremity gait dynamics: An introductory study. *Journal of Strength and Conditioning Research, 27*(6), 1503–1510.
Chung, M.-j., & Wang, M.-j. J. (2010). The change of gait parameters during walking at different percentage of preferred walking speed for healthy adults aged 20 – 60 years. *Gait & Posture, 31*(1), 131–135.
Dierick, F., Nivard, A. L., White, O., & Buisseret, F. (2017). Fractal analyses reveal independent complexity and predictability of gait. *Public Library of Science ONE, 12*(11), e0188711.
Dingwell, J. B., & Cusumano, J. P. (2000). Nonlinear time series analysis of normal and pathological human walking. *Chaos, 10*(4), 848–863.
Dingwell, J. B., & Cusumano, J. P. (2010). Re-interpreting detrended fluctuation analyses of stride-to-stride variability in human walking. *Gait & Posture, 32*(3), 348–353.
Dingwell, J. B., & Cusumano, J. P. (2015). Identifying stride-to-stride control strategies in human treadmill walking. *Public Library of Science ONE, 10*(4), e0124879.
Dingwell, J. B., & Marin, L. C. (2006). Kinematic variability and local dynamic stability of upper body motions when walking at different speeds. *Journal of Biomechanics, 39*(3), 444–452.
Dingwell, J. B., Salinas, M. M., & Cusumano, J. P. (2017). Increased gait variability may not imply impaired stride-to-stride control of walking in healthy older adults. *Gait & Posture, 55*(1), 131–137.
Diniz, A., Wijnants, M. L., Torre, K., Barreiros, J., Crato, N., Bosman, A. M. T., ... Delignières, D. (2011). Contemporary theories of 1/f noise in motor control. *Human Movement Science, 30*(5), 889–905.
Faisal, A. A., Selen, L. P., & Wolpert, D. M. (2008). Noise in the nervous system. *Nature Reviews Neuroscience, 9*(4), 292–303.
Garcia, M., Chatterjee, A., Ruina, A., & Coleman, M. (1998). The simplest walking model: Stability, complexity, and scaling. *Journal of Biomechanical Engineering, 120*(2), 281–288.
Gates, D. H., Su, J. L., & Dingwell, J. B. (2007). Possible biomechanical origins of the long-range correlations in stride intervals of walking. *Physica A: Statistical Mechanics and its Applications, 380*, 259–270.
Hausdorff, J. M. (2007). Gait dynamics, fractals and falls: Finding meaning in the stride-to-stride fluctuations of human walking. *Human Movement Science, 26*(4), 555–589.
Hausdorff, J. M., Peng, C.-K., Ladin, Z., Wei, J. Y., & Goldberger, A. L. (1995). Is walking a random walk? Evidence for long-range correlations in stride interval of human gait. *Journal of Applied Physiology, 78*(1), 349–358.
Hausdorff, J. M., Rios, D. A., & Edelberg, H. K. (2001). Gait variability and fall risk in community-living older adults: A 1-year prospective study. *Archives of Physical Medicine and Rehabilitation, 82*(8), 1050–1056.
Hollman, J. H., Watkins, M. K., Imhoff, A. C., Braun, C. E., Akervik, K. A., & Ness, D. K. (2015). A comparison of variability in spatiotemporal gait parameters between treadmill and overground walking conditions. *Gait & Posture, 43*, 204–209.
Ihlen, E. A. F. (2012). Introduction to multifractal detrended fluctuation analysis in Matlab. *Frontiers in Physiology, 3*, 141.
Jordan, K., Challis, J. H., & Newell, K. M. (2007). Walking speed influences on gait cycle variability. *Gait & Posture, 26*(1), 128–134.
Kang, H. G., & Dingwell, J. B. (2008). Separating the effects of age and walking speed on gait variability. *Gait & Posture, 27*(4), 572–577.
Lancaster, G., Iatsenko, D., Pidde, A., Ticcinelli, V., & Stefanovska, A. (2018). Surrogate data for hypothesis testing of physical systems. *Physics Reports, 748*, 1–60.
Martin, A. E., Villarreal, D. J., & Gregg, R. D. (2016). Characterizing and modeling the joint-level variability in human walking. *Journal of Biomechanics, 49*(14), 3298–3305.
McGinley, J. L., Baker, R., Wolfe, R., & Morris, M. E. (2009). The reliability of three-dimensional kinematic gait measurements: A systematic review. *Gait & Posture, 29*(3), 360–369.
Moon, Y., Sung, J. H., An, R., Hernandez, M. E., & Sosnoff, J. J. (2016). Gait variability in people with neurological disorders: A systematic review and meta-analysis. *Human Movement Science, 47*(1), 197–208.
Nelson, J. D. B., Nafornita, C., & Isar, A. (2015). Generalised M-lasso for robust, spatially regularised Hurst estimation. *2015 IEEE Global Conference on Signal and Information Processing* (pp. 1265–1269). .
O'Connor, C. M., Thorpe, S. K., O'Malley, M. J., & Vaughan, C. L. (2007). Automatic detection of gait events using kinematic data. *Gait and Posture, 25*(3), 469–474.
Rhea, C. K., Kiefer, A. W., D'Andrea, S. E., Warren, W. H., & Aaron, R. K. (2014). Entrainment to a real time fractal visual stimulus modulates fractal gait dynamics. *Human Movement Science, 36*, 20–34.
Roerdink, M., Daffertshofer, A., Marmelat, V., & Beek, P. J. (2015). How to sync to the beat of a persistent fractal metronome without falling off the treadmill? *Public Library of Science ONE, 10*(7), e0134148.
Roerdink, M., de Jonge, C. P., Smid, L. M., & Daffertshofer, A. (2019). Tightening up the control of treadmill walking: Effects of maneuverability range and acoustic pacing on stride-to-stride fluctuations. *Frontiers in Physiology, 10*, 257.
Schreiber, T., & Schmitz, A. (2000). Surrogate time series. *Physica D: Nonlinear Phenomena, 142*(3–4), 346–382.
Schwartz, M. H., Rozumalski, A., & Trost, J. P. (2008). The effect of walking speed on the gait of typically developing children. *Journal of Biomechanics, 41*(8), 1639–1650.
Sinha, A. (2010). *Vibration of mechanical systems.* Cambridge University Press.
Vicon (2018a). *Plug-in gait reference guide*.
Vicon (2018b). *Vicon nexus user guide*.
Warlop, T., Detrembleur, C., Stoquart, G., Lejeune, T., & Jeanjean, A. (2018). Gait complexity and regularity are differently modulated by treadmill walking in Parkinson's disease and healthy population. *Frontiers in Physiology, 9*, 68.
Yamasaki, M., Sasaki, T., & Torii, M. (1991). Sex difference in the pattern of lower limb movement during treadmill walking. *European Journal of Applied Physiology and Occupational Physiology, 62*(2), 99–103.
Zajac, F. E. (1989). Muscle and tendon: Properties, models, scaling, and application to biomechanics and motor control. *Critical Reviews in Biomedical Engineering, 17*(4), 359–411.
Zhang, J., Zhang, K., Feng, J., & Small, M. (2010). Rhythmic dynamics and synchronization via dimensionality reduction: Application to human gait. *Public Library of Science Computational Biology, 6*(12), e1001033.